

Stopping power and effective charge of heavy ions in solids

J. M. Anthony*

*A. W. Wright Nuclear Structure Laboratory,
Yale University, New Haven, Connecticut 06511*

W. A. Lanford

*Department of Physics,
SUNY at Albany, Albany, New York 12222
(Received 17 August 1981)*

We have measured the energy loss of several heavy ions (C, Si, Cl, Ti, Fe, Ni, Ge, Br, Nb, and I) in elemental targets (C, Al, Cu, Ag, and Au) at energies near the maximum in the stopping power versus energy curve. These measurements have been used to examine the charge dependence of heavy-ion stopping powers, as well as the magnitude of the ion's effective charge inside the target material. Inclusion of the Lindhard Z_1^3, Z_1^4 corrections provides the best fit to the data, and the use of these corrections results in a simple expression for the effective charge which is valid for all our measured projectile-target combinations ($Z_1=6-53$ and $Z_2=6-79$). Both the magnitude and the target dependence of this effective-charge expression are consistent with average equilibrium charge-state measurements made in gases. This suggests that the high charge states observed for ions leaving solid materials are due mainly to charge-changing effects (such as Auger deexcitation) at the exit surface.

I. INTRODUCTION

Although the equilibrium charge states of energetic heavy ions after passing through solid media have been measured extensively,¹ there is still considerable uncertainty about the charge states of the ions while they are inside the target material. For a given ion beam, the measured charge states of ions exiting solid targets are much higher than those found for gaseous targets. Betz,² *et al.* suggest that this difference is due to emission of Auger electrons at the exit surface, but that the charge states *inside* solids and gases of the same atomic number are approximately the same. Any attempt to calculate these charge states is complicated, however, by the large number of electron capture and loss cross-sections involved.

One obvious way to examine the charge states of heavy ions inside solids is to study the stopping power of these ions, which depends directly on the projectile charge. The usefulness of any effective charge expression derived from dE/dx measurements is limited, however, by the accuracy of the stopping-power theory used to describe the data. (We define effective charge to be the charge which is calculated from experimental dE/dx measure-

ments by using a particular stopping-power theory.) Most current stopping-power tabulations^{3,4} assume that the energy-loss process is proportional to the square of the projectile charge. This results in an effective charge which, although quite similar in magnitude to average equilibrium charge-state measurements in gases, shows no target dependence. Recent energy-loss measurements⁵⁻⁸ suggest that higher-order charge-dependent corrections to the stopping power are important; the inclusion of these corrections will influence the effective charge deduced from the data. One constraint on these calculated effective-charge states is that they should exhibit approximately the same target behavior as equilibrium charge-state measurements.

In order to investigate both the general behavior of the higher-order dE/dx corrections, as well as the projectile effective charge, we have measured the energy loss of 10 heavy ions (C, Si, Cl, Ti, Fe, Ni, Ge, Br, Nb, and I) in five target materials (C, Al, Cu, Ag, and Au) at energies near the maximum in the stopping power versus energy curve. Since these two effects cannot be examined separately, a large data base was necessary to test the generality of the results and also to reduce the in-

fluence of random errors in any particular projectile-target combination. Several expressions for the energy-loss process, both with and without the higher-order corrections, have been examined, along with various effective charge parametrizations. The results are compared with previous determinations of the higher-order dE/dx corrections, as well as average equilibrium charge-state measurements for ions exiting solids and gases.

An alternate approach for determining the influence of higher-order charge effects is to measure energy losses in a channeling geometry, which in some cases allows preservation of the ion charge state during penetration. The recent results of Golovchenko *et al.*²⁰ using this method seem not to need higher-order effects. However, this may be due to cancellation of higher-order terms for the particular ions ($Z_1=9-17$) and energies ($E \approx 3$ MeV/amu) measured, and thus it is difficult to determine if these results are in conflict with the present conclusions.

II. EXPERIMENTAL PROCEDURE

The apparatus used for these stopping-power measurements is shown in Figs. 1 and 2. The incident heavy-ion beam from the Yale MP tandem accelerator passed through three collimating slits and into a thin gold foil at the center of the scattering chamber. Most of the incident beam was undeflected, and it passed through the annulus containing the detectors (Fig. 2) and directly into the Faraday cup. Ten silicon surface barrier detectors were mounted in the annulus which was placed approximately eleven inches downstream from the gold scattering foil. Beam particles scat-

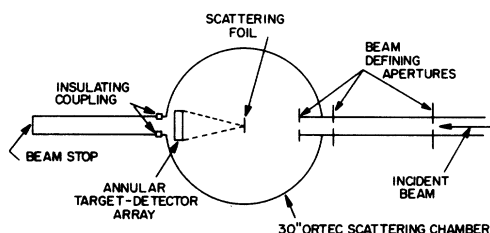


FIG. 1. Schematic representation of the experimental apparatus. The heavy-ion beam, incident from the right, passes through three collimating slits and into the Au scattering foil. Part of the beam particles are elastically scattered to 10° and into detectors mounted on the annulus—the main portion of the beam is undeflected and passes through the hole in the annulus and into the beam dump.

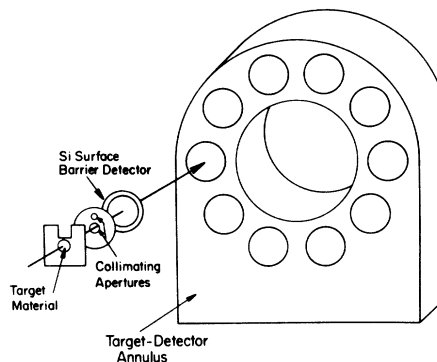


FIG. 2. Target-detector annulus. Particles scattered to 10° by the Au foil (Fig. 1) pass directly into ten target-collimators-detector arrangements mounted on an annular ring. The geometry shown allows the detector to collect (1) particles suffering energy loss by passing directly through the target material (large hole in collimator) and (2) particles not going through the target and therefore experiencing no energy loss (small hole in collimator).

tered by the gold foil to 10° were then collected in all ten detectors simultaneously. A self-supporting evaporated target and a circular collimating aperture (with an area ~ 12 mm²) were mounted in front of each detector. The collimating aperture was ~ 2 mm behind the target. The target frames and collimators were designed so that each detector collected both (1) particles passing through the target material and into the detector and (2) particles passing directly into the detector without going through the target. The particles not passing through the target thus entered the detector at essentially the beam energy (with a small correction due to 10° scattering from the gold foil). This provided an energy calibration for each beam and each detector, while the energy losses were being measured. Each detector output was sent into a separate multichannel analyzer, and the resulting spectra each had two peaks corresponding to the ions which did and did not pass through the target. Thus the difference between peak locations (as determined by a computer peak fitting routine), when coupled with the calibration curve for that particular detector, gave a direct measure of the energy loss in the target.

These self-supporting targets were all prepared commercially by vacuum evaporation (Micromatter Co.). Data were taken for two samples of each material in an attempt to avoid possible systematic errors reflecting inaccuracies in target thickness determinations. The thicknesses of these targets were measured using several methods, including (1)

weighing, (2) Rutherford backscattering of α particles at 2 MeV, and (3) energy loss of ^{228}Th α particles at 5–9 MeV. α -particle backscattering was also used to test the uniformity of these targets, which was better than 1% in all cases. The ^{228}Th α -particle measurements were made using exactly the same geometry and analysis techniques as the heavy-ion measurements. The stopping power of α particles in this energy range has been very accurately measured for Al, Cu, Ag, and Au, targets,⁵ and this procedure thus yielded very precise values for our target thickness. The results for all three techniques (weighing, α -particle backscattering, and α -particle energy loss) were consistent with one another in all cases. Table I lists these target thicknesses.

III. ANALYSIS AND RESULTS

While the contribution of nuclear stopping is quite small for the energy losses reported here, we have used the results of Ref. 9 to estimate nuclear stopping and have subtracted these values from the total energy losses. The results of these measurements are shown in Figs. 3–7. Current heavy-ion stopping power and range compilations include those of Northcliffe (NS)³ and Ziegler,⁴ and their values are also shown. In general, the standard tabulations do poorly in predicting the magnitude and the location of the stopping power maximum for the projectile-target combinations which we have studied. The behavior of all our heavy-ion measurements in a given target material is fairly consistent; in Ag targets, for example, the peak is almost always (1) larger in magnitude, and (2) lower in energy than the standard predictions.

TABLE I. Targets used in our energy-loss measurements.

Target material	Thickness ($\mu\text{g}/\text{cm}^2$)
C	105 ± 2.4
C	98 ± 3
Al	252 ± 4.5
Al	247 ± 4
Cu	382 ± 5
Cu	387 ± 6
Ag	365 ± 6
Ag	396 ± 5
Au	614 ± 10
Au	623 ± 11

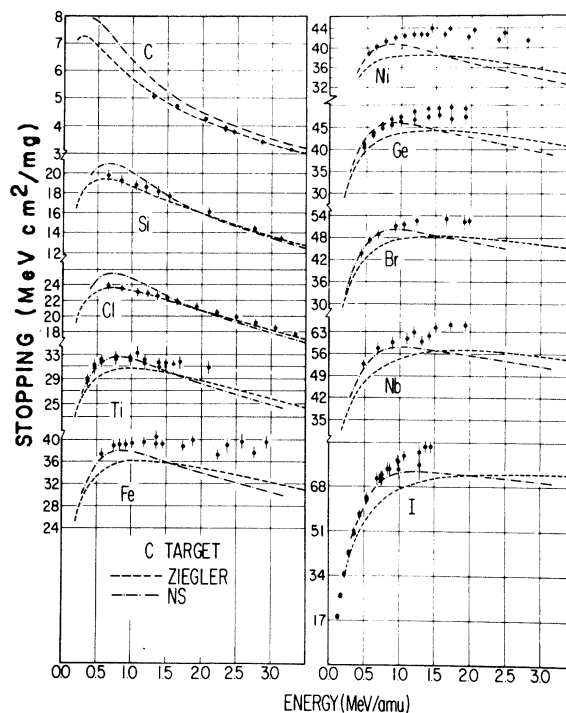


FIG. 3. Electronic stopping power of all our heavy ions ($Z_1=6-53$) in C, vs energy. Also shown are the predictions of Ziegler (---) and NS (-·-·-·).

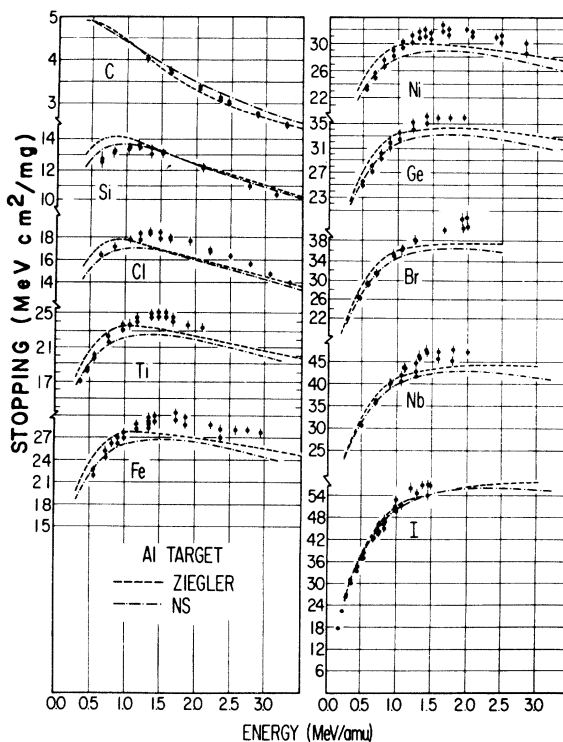


FIG. 4. Electronic stopping power of all our heavy ions ($Z_1=6-53$) in Al vs energy. Also shown are the predictions of Ziegler (---) and NS (-·-·-·).

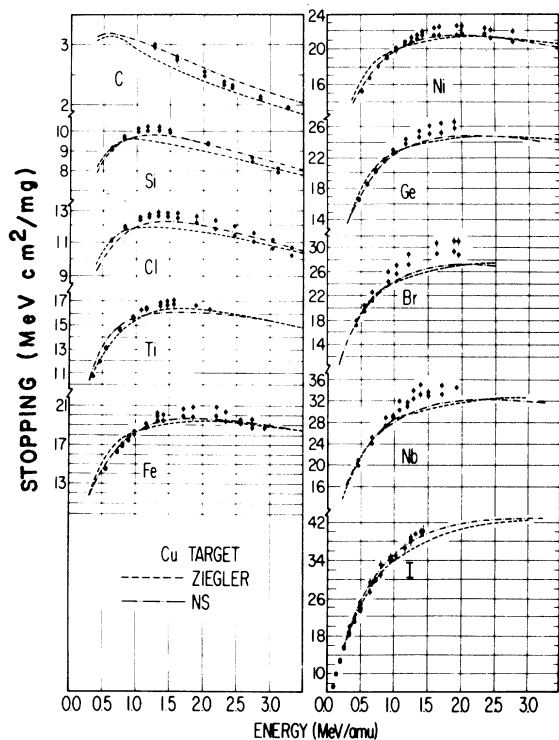


FIG. 5. Electronic stopping power of all our heavy ions ($Z_1=6-53$) in Cu vs energy. Also shown are the predictions of Ziegler (---) and NS (-·-·-·).

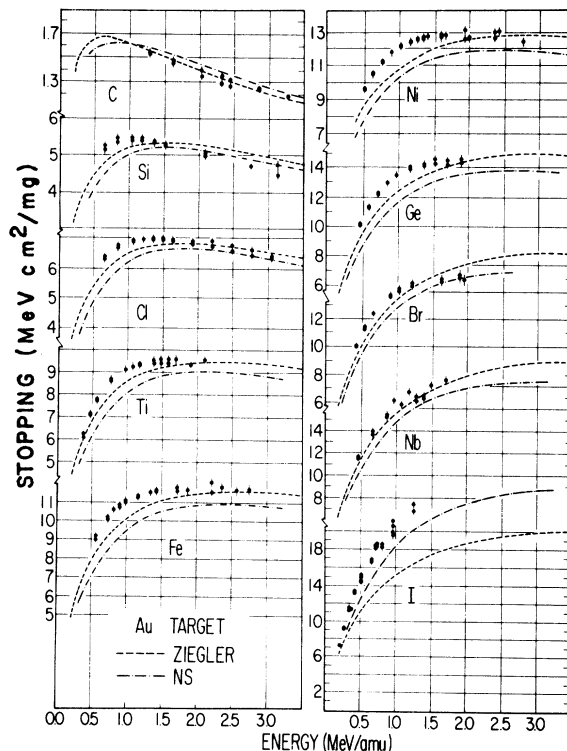


FIG. 7. Electronic stopping power of all our heavy ions ($Z_1=6-53$) in Au vs energy. Also shown are the predictions of Ziegler (---) and NS (-·-·-·).

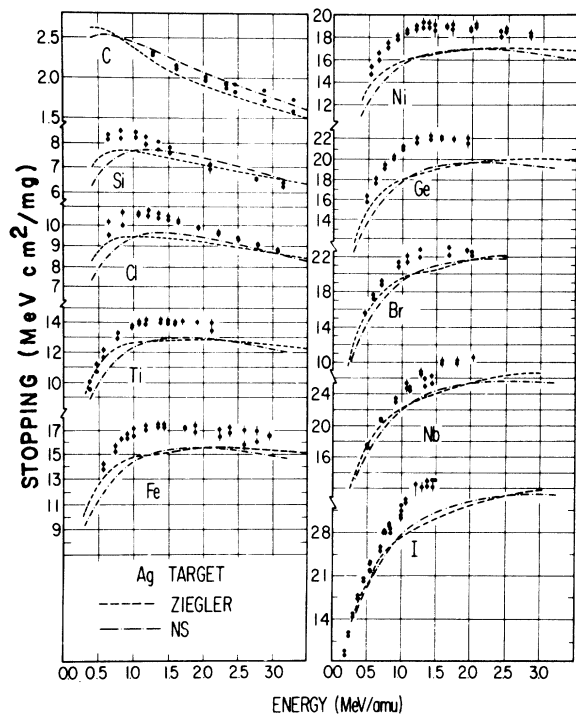


FIG. 6. Electronic stopping power of all our heavy ions ($Z_1=6-53$) in Ag vs energy. Also shown are the predictions of Ziegler (---) and NS (-·-·-·).

Figures 8 and 9 show the ratio of our dE/dx measurements in Ag targets to the predictions of Ziegler and NS, plotted versus the ion energy. This demonstrates more clearly the consistent

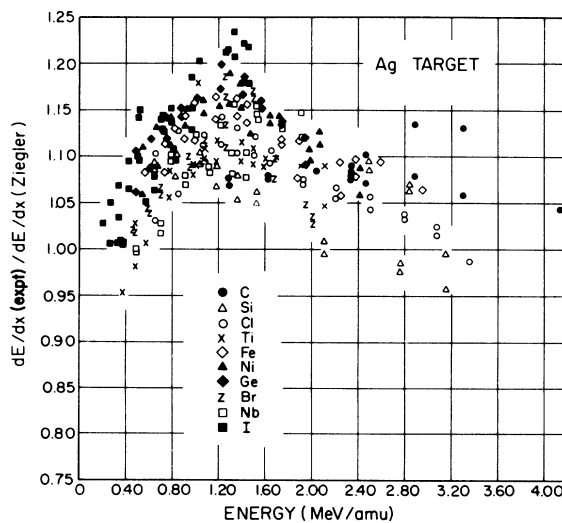


FIG. 8. Ratio of all our experimental energy-loss measurements in Ag targets to the predictions of Ziegler versus energy.

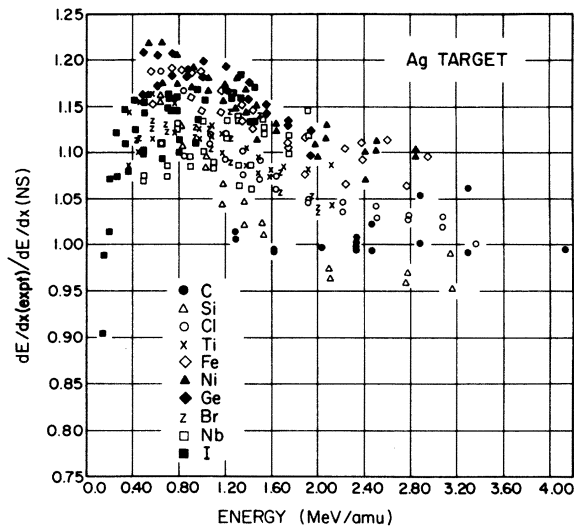


FIG. 9. Ratio of all our experimental energy-loss measurements in Ag targets to the predictions of NS versus energy.

behavior of all our measurements in a given target material.

The systematic discrepancies in Figs. 3–9 call into question the charge dependence used in producing the standard tabulations. The energy loss in this velocity region, for a projectile of charge Z_1e and velocity $v = \beta c$ passing through a target material of charge Z_2e is usually written as

$$-\frac{dE}{dx} = C \frac{Z_1^2}{\beta^2} L,$$

where

$$C = \left[\frac{4\pi N_0 e^4 Z_2}{mc^2 A_2} \right] = 3.07 \times 10^{-4} \frac{Z_2}{A_2}$$

in units of MeV cm²/mg, and the stopping number L depends on the particular theory used to describe the energy loss. Both Ziegler and NS assume $L = L_0(v, Z_2)$, i.e., it depends only on target material and projectile velocity, which results in a simple Z_1^2 stopping-power dependence. Recent measurements^{5–8} suggest, however, that corrections to this scaling are necessary, and several expressions^{8,10,11,12} have been advanced to evaluate these corrections. Comparisons of these expressions with experiments on heavy ions are complicated, however, by lack of knowledge about the charge state of the ion inside the target material. Although average charge states of heavy ions passing through gaseous targets are believed to be the same both inside and outside the gas, there is some

debate about the importance of charge-changing effects as the ions exit the surface of solid materials, and thus the magnitude of projectile charges inside solids is not well known. Both solid and gas targets generate the same target dependence in heavy-ion charge states, however, in that low- Z_2 targets produce higher projectile charges than high- Z_2 targets, and this target dependence is a constraint on the effective charge values deduced from energy loss measurements.

Both the Ziegler and NS tabulations assume a Z_1^2 stopping-power dependence. If this form is used, a ratio of experimental dE/dx values for two different heavy ions, measured in the same target material and at the same velocity, will give a value for the square of the ratio of the two heavy-ion effective charges, i.e.,

$$\frac{(dE/dx)_A}{(dE/dx)_B} = \frac{Z_{1A}^{*2}}{Z_{1B}^{*2}},$$

where Z_1^* is the effective charge of a projectile of atomic number Z_1 and A and B represent the two ions under consideration. If one of the ions is chosen to be hydrogen, and the measurements are made at velocities large enough so that the proton is stripped of its electron, then the hydrogen effective charge is equal to one and we have a direct measure of the heavy-ion effective charge. This technique has been used by many workers,^{3,4,13} but the resultant effective-charge expressions show no target dependence, which is at variance with the constraint discussed above. This suggests that the Z_1^2 stopping-power dependence may not be complete.

In Figs. 10 and 12 we have analyzed our energy-loss measurements for Si and Br ions assuming a Z_1^2 stopping-power dependence. Values of the ion effective charge were calculated from the ratio of our data to proton stopping powers, which have been very accurately measured for the four materials shown.⁵ In each case the velocities are high enough to ensure that the proton is stripped. The resultant effective-charge values (divided by the ion atomic number) are plotted versus the ion velocity. Values for the C data have not been calculated, since the dE/dx measurements for protons in C are not as well known as in the other materials. There is no simple target dependence evident in these values, and thus the Z_1^2 stopping-power dependence does not allow our data to reproduce the target dependence of equilibrium charge states of ions exiting materials.

We have also analyzed the same data by includ-

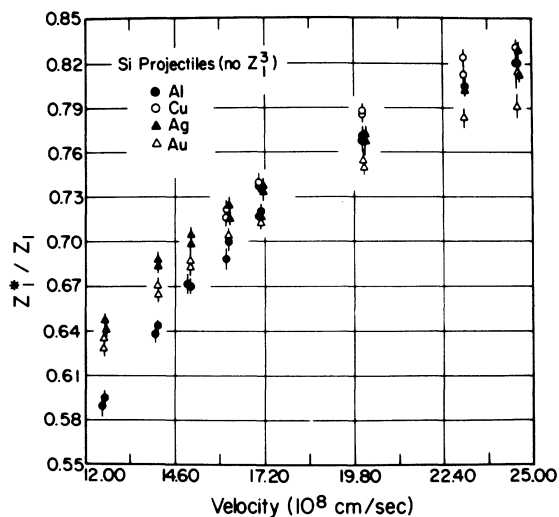


FIG. 10. Values of the effective charge of Si ions (divided by the atomic number of Si), calculated from experimental dE/dx measurements by assuming a Z_1^3 stopping-power dependence versus velocity.

ing higher-order charge-dependent corrections to the stopping power. In this case no simple ratio will provide values for the effective charge, and we must assume some particular theory. We have utilized the corrections of Lindhard¹⁰ in which the stopping number L can be written

$$L = L_0(v, Z_2) + Z_1 L_1(v, Z_2) + \Phi(v, Z_1) .$$

Lindhard suggests a Z_1^3 term [$L_1(v, Z_2)$] approximately twice that of Jackson and McCarthy,¹² and

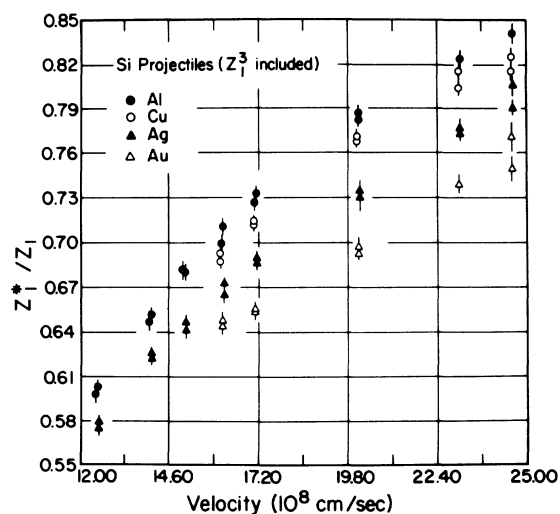


FIG. 11. Values of the effective charge of Si ions (divided by the atomic number of Si), calculated from experimental dE/dx measurements by including the higher-order corrections of Lindhard versus velocity.

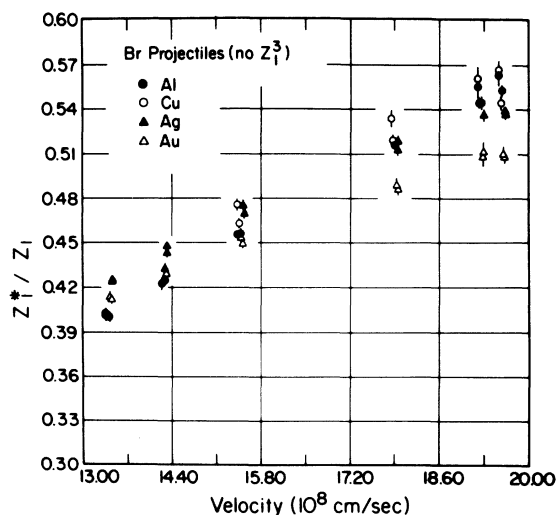


FIG. 12. Values of the effective charge of Br ions (divided by the atomic number of Br), calculated from experimental dE/dx measurements by assuming a Z_1^3 stopping-power dependence versus velocity.

we have calculated L_1 assuming twice their tabulated values. The term $\Phi(v, Z_1)$ was originally proposed by Bloch,¹⁴ and is given by

$$\Phi(v, Z_1) = -y^2 \sum_{n=0}^{\infty} \frac{1}{n(n^2 + y^2)} ,$$

where $y = Z_1 V_0 / V$ with $V_0 = e^2 / \hbar$.

Values for $L_0(v, Z_2)$ have been determined experimentally by Andersen *et al.*⁵ to high accuracy for the targets shown (accurate data for C targets are

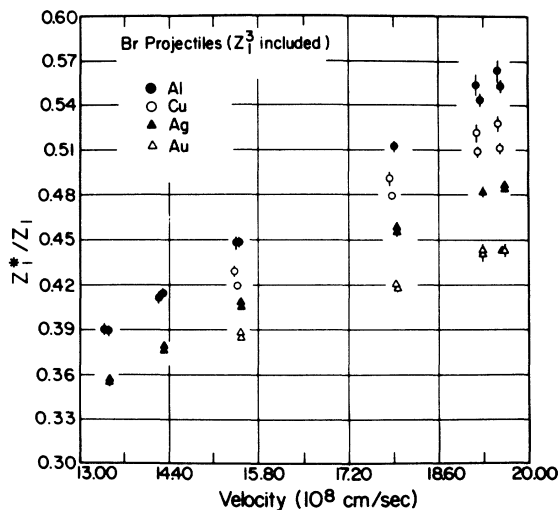


FIG. 13. Values of the effective charge of Br ions (divided by the atomic number of Br), calculated from experimental dE/dx measurements by including the higher-order corrections of Lindhard versus velocity.

not available), and consequently we have used their values for L_0 . Since our calculations are based on the experimental work of Andersen *et al.*, we go no lower in velocity than their measurements, i.e., $E \sim 1.0$ MeV/amu. As before, we must substitute Z_1^* for Z_1 , since the heavy ions are not fully stripped. Thus, in the above expression for L , all terms except the ion effective charge are known, and this effective charge can be computed iteratively from our dE/dx measurements. The results of these calculations are shown in Figs. 11 and 13. In each case, use of the higher-order corrections allows our calculated effective charge values to reproduce the expected target dependence. This effect is true of all our heavy ion data, and is not peculiar to Si and Br.

The success of this procedure suggests that a general expression for heavy-ion effective charge may be possible. However, some assumptions about the form of this effective charge expression

are necessary. Previously the average equilibrium charge states \bar{Z}_1 have been fit with a semiempirical formula given by

$$\frac{\bar{Z}_1}{Z_1} = 1 - A \exp \left[\frac{-\lambda v}{v_0 Z_1^\gamma} \right],$$

where various combinations of A , λ , and γ are used as search parameters. We have substituted Z_1^* for \bar{Z}_1 in the above expression and used it, in conjunction with the various higher-order stopping-power corrections, in an attempt to provide a fit to our heavy-ion energy-loss measurements. A Thomas-Fermi statistical description of the target atom suggests $\gamma = \frac{2}{3}$,^{15,16} and we have adopted this value in our fits, leaving A and λ as free parameters. (Other combinations of A , λ , and γ as free parameters have also been tried, but with less success.) The target dependence of the effective charge implies that a separate fit is necessary for each target material. However, due to the systematic behavior

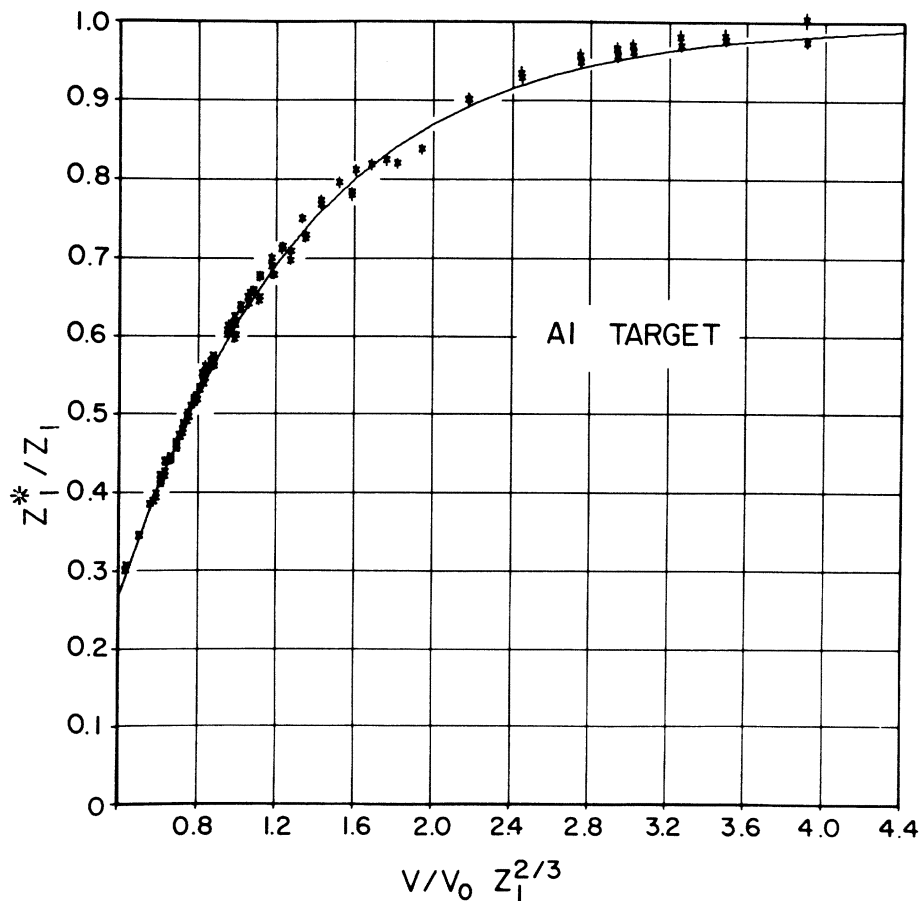


FIG. 14. Values of the effective charge of all our heavy ions (divided by the ion atomic number Z_1) in Al, calculated from experimental dE/dx measurements by including the higher-order corrections of Lindhard versus the reduced velocity $V/V_0 Z_1^{2/3}$. Also shown is our two-parameter effective-charge fit for Cu (—).

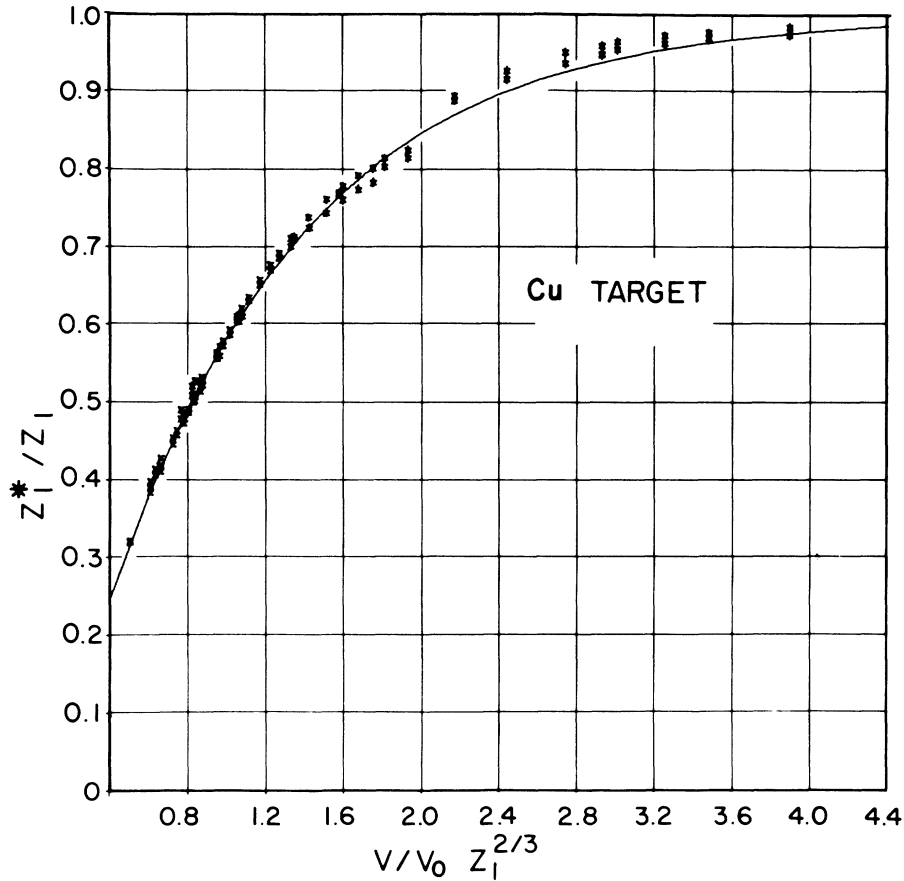


FIG. 15. Values of the effective charge of all our heavy ions (divided by the ion atomic number Z_1) in Cu, calculated from experimental dE/dx measurements by including the higher-order corrections of Lindhard versus the reduced velocity $V/V_0 Z_1^{2/3}$. Also shown is our two-parameter effective-charge fit for Cu (—).

of all our heavy ions in a given target, as illustrated in Figs. 3–9, we have attempted to fit our energy-loss measurements in that target, ranging from C ions to I ions with *one* set of values for A and λ . Three different forms for the higher-order corrections have been examined, including (1) Lindhard,¹⁰ (2) Anderson *et al.*,⁵ and (3) Ashley, Ritchie, and Brandt,^{11,17} where the corrections of Ashley *et al.* have one additional adjustable parameter. Thus we have used at most three parameters for each target, two for the effective-charge expression, and one for the higher-order corrections of Ashley *et al.* to fit all our heavy-ion energy-loss measurements, which vary over a wide range of energies (0.5–4.0 MeV/amu) and projectile atomic numbers ($Z_1=6$ to 53).

The stopping-power corrections that provide the best fit to our data are those of Lindhard. These higher-order terms, in conjunction with the two-parameter effective-charge expression discussed

above, allow accurate fits to all our data in Al, Cu, Ag, and Au targets. This is consistent with the results of other workers,^{5,7} who also find that the Lindhard corrections provide good fits to their data. Andersen *et al.*⁵ used their measurements for p , α , and Li projectiles in Al, Cu, Ag, and Au to separate out Z_1^3 and Z_1^4 effects consistent with the corrections of Lindhard, while the results of Heckman and Lindstrom,⁶ on the stopping-power difference between π^+ and π^- particles, are well described by the Lindhard results. In Figs. 14–17 we have calculated projectile effective charges for all our ions, using the stopping-power terms of Lindhard, and plotted them versus the reduced velocity, given by $V_r = V/V_0 Z_1^{2/3}$. Also shown is the two-parameter effective-charge expression for each target, and these curves are seen to fit the extracted Z_1^* values over a broad range.

The success of our fits can also be examined directly. Using the values for A and λ in Ag tar-

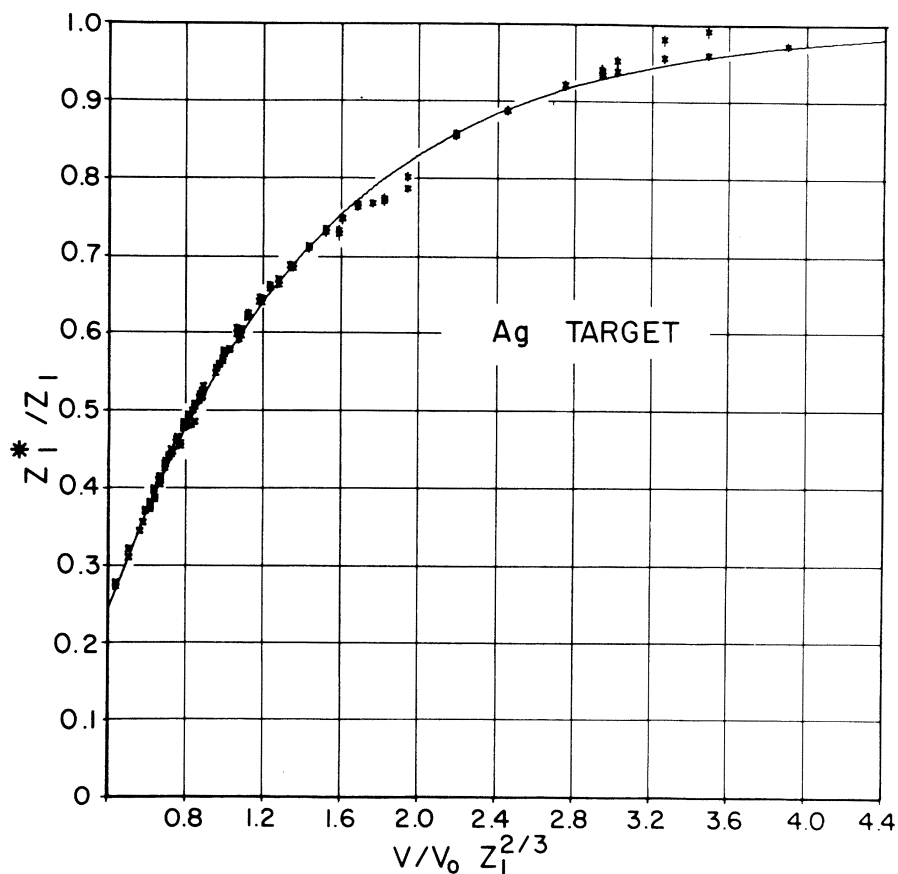


FIG. 16. Values of the effective charge of all our heavy ions (divided by the ion atomic number Z_1) in Ag, calculated from experimental dE/dx measurements by including the higher-order corrections of Lindhard versus the reduced velocity $V/V_0 Z_1^{2/3}$. Also shown is our two-parameter effective-charge fit for Ag (—).

gets as determined by our fitting techniques, we can generate an effective-charge expression which, when coupled with the Lindhard higher-order corrections, allows us to predict the energy loss for all our heavy-ion measurements in Ag targets. To illustrate this, we have taken the ratio of our experimental measurements to the predictions of our two-parameter fit and plotted these versus the ion energy (Fig. 18). This technique produces substantially better results than the standard tabulations, and can reproduce essentially all our data at the 5% level. Similar results are found in Al, Cu, and Au targets, as well. Moreover, the systematic discrepancy between prediction and experiment, as shown in Figs. 8 and 9, has been reduced considerably.

Although there is no strong initial motivation for the values of the two parameters A and λ in the effective-charge parametrization used here, the ability of this expression to fit our data suggests

that there may be some physical justification for them. Figure 19 shows the values of these parameters as determined by our fits, plotted versus the target atomic number, while Table II gives the values of these parameters. Both A and λ can be described by a simple quadratic expression, i.e.,

$$A = 1.16 - 1.91 \times 10^{-3} Z_2 + 1.26 \times 10^{-5} Z_2^2$$

and

$$\lambda = 1.18 - 7.5 \times 10^{-3} Z_2 + 4.53 \times 10^{-5} Z_2^2$$

and these curves are also shown in Fig. 19. The smooth behavior of these parameters may allow interpolation between our measured values, and the resultant effective-charge expression can then be coupled with the Lindhard corrections to produce energy-loss curves for projectile-target combinations not covered in this paper. However, since the targets in the present study do not include those

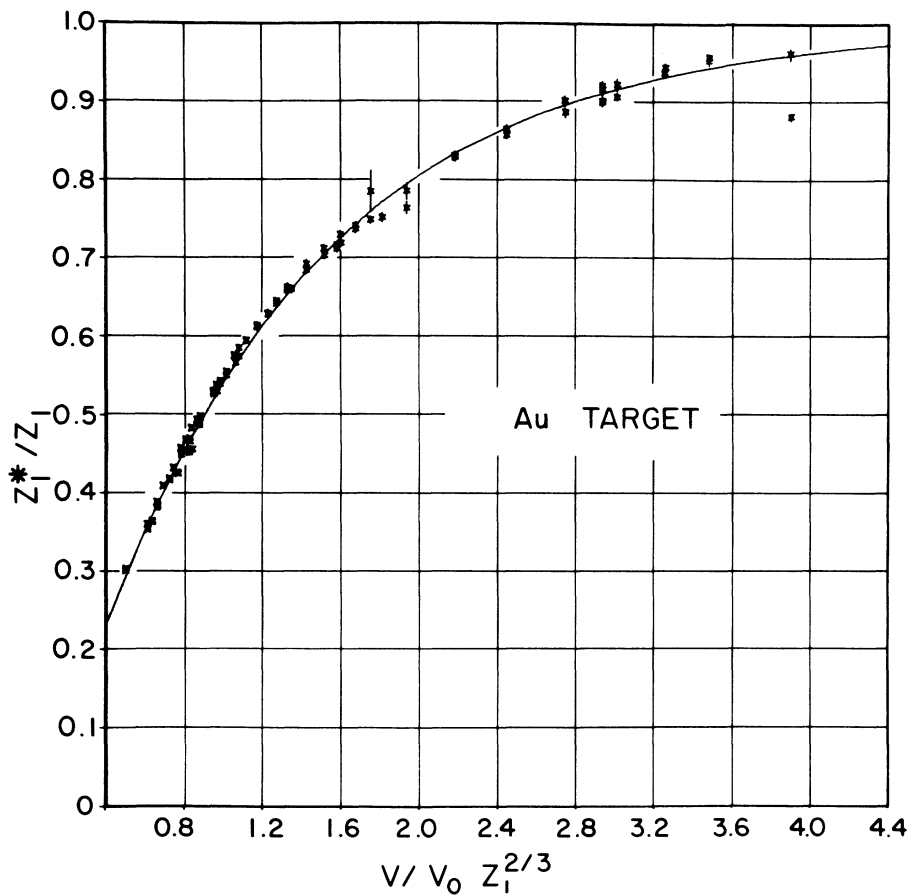


FIG. 17. Values of the effective charge of all our heavy ions (divided by the ion atomic number Z_1) in Au, calculated from experimental dE/dx measurements by including the higher-order corrections of Lindhard versus the reduced velocity $V/V_0 Z_1^{2/3}$. Also shown is our two-parameter effective-charge fit for Au (—).

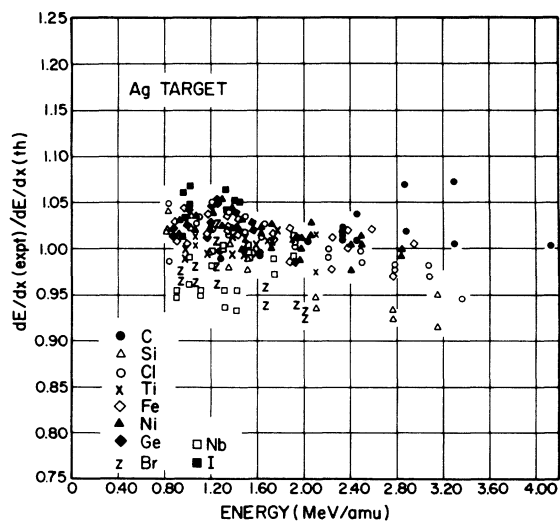


FIG. 18. Ratio of all our experimental energy-loss measurements in Ag targets to the predictions of the present study (—).

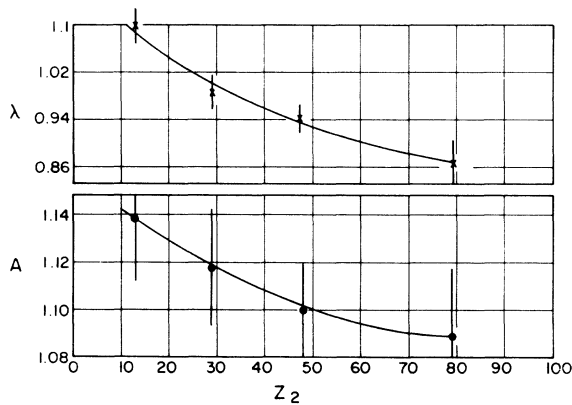


FIG. 19. Values of the two parameters A and λ in our effective-charge expression versus target atomic number. The solid curves represent a quadratic dependence on Z_2 .

TABLE II. Effective-charge parameters.

Target atomic number	A	λ
13	1.139	1.099
29	1.117	0.984
47	1.10	0.942
79	1.09	0.869

displaying the full range of shell structure, the possibility of shell effects in our charge-state parameters should be considered.

The values of A and λ shown here demonstrate that the effective-charge expression has a strong target dependence for all velocities, consistent with equilibrium charge-state measurements. Furthermore, the magnitude of the effective charges calculated using this expression are very close to average equilibrium charge-state measurements in gases,¹ thus supporting the idea that charge states inside solids and gases are approximately the same, but that near surface effects, such as the emission of Auger electrons by projectiles after leaving solid surfaces, result in high values of ionization. Independent calculations on electron capture and loss cross sections by Betz *et al.*² also support this idea. Thus a comparison of our effective-charge values calculated inside the solid with average equilibrium charge-state measurements outside may give a measure of the number of Auger electrons emitted by the projectile near the solid surface. Based on current data for average charge states of heavy ions exiting solid foils,^{18,19} the number of these electrons should vary over a broad range, from ~ 2 for 10 MeV sulfur in gold, for example, to about 10 for 180 MeV iodine in aluminum.

IV. CONCLUSIONS

We have reported energy-loss measurements for 10 heavy ions in five target materials over a broad

energy range. The results of these measurements are not well described by current standard tabulations, and higher-order charge-dependent corrections to the stopping power are necessary. Several forms for these higher-order corrections have been examined, in conjunction with various effective-charge parametrizations. The best fits to our data are provided by corrections proposed by Lindhard, together with a simple two-parameter expression which describes heavy-ion effective charges for all the ions in a given target. Use of this charge parametrization, when coupled with the Lindhard corrections, allows prediction of dE/dx values with much better success than the standard tabulations, which assume a Z_1^2 stopping-power dependence.

The effective-charge expression generates heavy-ion effective-charge values which agree well both in magnitude and in target dependence with equilibrium charge-state measurements in gases. This suggests that charge states inside solids and gases (of approximately the same atomic number) are almost the same, and that the high charge states of ions when leaving solids may be due to processes such as loss of Auger electrons at the exit surface of the solid. Comparison of average equilibrium charge states with our effective charge expression may thus give a measure of the number of Auger electrons emitted by the projectile upon leaving the solid surface.

ACKNOWLEDGMENT

This work was supported in part by the U.S. Department of Energy under Contract No. DE-AC02-76ER03074. W. A. L. acknowledges fellowship assistance from the Alfred P. Sloan Foundation.

*Present address: Materials Characterization Laboratory, Texas Instruments, Inc., P.O. Box 225936, MS 147, Dallas, Texas 75265.

¹H. D. Betz, *Rev. Mod. Phys.* **44**, 465 (1972).

²H. D. Betz, *Nucl. Instrum. and Methods* **132**, 19 (1976).

³L. C. Northcliffe and R. F. Schilling, *Nucl. Data Tables* **A7**, 233 (1970).

⁴J. F. Ziegler, *Handbook of Stopping Cross Sections for Energetic Ions in all Elements* (Pergamon, New York,

1980).

⁵H. H. Andersen, J. F. Bak, H. Knudsen, B. R. Nielsen, *Phys. Rev.*, A **16**, 1929 (1977).

⁶H. H. Heckman and P. J. Lindstrom, *Phys. Rev. Lett.* **22**, 871 (1969).

⁷J. M. Anthony and W. A. Lanford, *Nucl. Instrum. and Methods* **186**, 647 (1981).

⁸H. H. Andersen, H. Simonsen, and H. Sorensen, *Nucl. Phys.* **A125**, 171 (1969).

⁹J. F. Ziegler, *Appl. Phys. Lett.* **31**, 544 (1977).

- ¹⁰J. Lindhard, Nucl. Instrum. and Methods 132, 1 (1976).
- ¹¹R. H. Ritchie and W. Brandt, Phys. Rev. A 17, 2102 (1978).
- ¹²J. D. Jackson and R. L. McCarthy, Phys. Rev. B 6, 4131 (1972).
- ¹³G. D. Sauter and S. D. Bloom, Phys. Rev. B 6, 699 (1972).
- ¹⁴F. Bloch, Ann. Phys. 16, 285 (1933).
- ¹⁵N. Bohr, Kgl. Danske Videnskab. Selskab, Mat.-Fys. Medd. 18, No. 8 (1948).
- ¹⁶N. Bohr and J. Lindhard, Kgl. Danske Videnskab. Selskab, Mat.-Fys. Medd. 28, No. 7 (1954).
- ¹⁷J. C. Ashley, R. H. Ritchie, and W. Brandt, Phys. Rev. B 5, 2393 (1972).
- ¹⁸H. D. Betz, G. Hortig, E. Leischner, Ch. Schmelzer, B. Stadler, and J. Weihrauch, Phys. Lett. 22, 643 (1966).
- ¹⁹S. Datz, C. D. Moak, H. O. Lutz, L. C. Northcliffe, and L. B. Bridwell, At. Data 2, 273 (1971).
- ²⁰J. A. Golovchenko, A. N. Goland, J. S. Rosner, C. E. Thorn, H. E. Wegner, H. Knudsen, and C. D. Moak, Phys. Rev. B 23, 957 (1981).